coatings

MDPI

Article

The Influence of Alumina Airborne-Particle Abrasion on the Properties of Zirconia-Based Dental Ceramics (3Y-TZP)

Paulina Łagodzińska [1,*], Beata Dejak [1] and Bartłomiej Konieczny [2]

[1] Department of Prosthodontics, Medical University of Lodz, 90-419 Lodz, Poland
[2] University Laboratory of Material Research, Medical University of Lodz, 90-419 Lodz, Poland
* Correspondence: paulina.lagodzinska@umed.lodz.pl

Abstract: The objective of this study was to assess the effect of airborne-particle abrasion with alumina particles of various sizes (50 µm, 110 µm, 250 µm) on the surface properties of 3Y-TZP (3 mol% yttria-stabilized tetragonal zirconia polycrystals). The analysis comprised the Vickers hardness test (HV1kp), a surface roughness evaluation (Ra, Rq, Rz, Rsk, Rsm, Rt, Vo, profile displays), and SEM–EDS microanalysis (scanning electron microscopy–energy-dispersive X-ray spectroscopy). Any statistical relationships were assessed using the Kruskal–Wallis one-way analysis-of-variance-by-rank test ($p = 0.05$). While airborne-particle abrasion with 50 µm alumina significantly increases the Vickers hardness of 3Y-TZP (1678.8 HV1kp), 110 µm and 250 µm alumina particles do not appear to have any such effect. The surface roughness of 3Y-TZP increases with the size of the alumina particles (Ra, Rq, Rz, Rt, Vo: vertical plane and retention volume assessment); a higher Rsm (horizontal plane assessment) was noted for specimens air-abraded with 250 µm alumina particles; air abrasion with 50 µm alumina particles yielded a symmetrical surface roughness profile (Rsk). The major topographic pattern of the surface of 3Y-TZP is altered by alumina airborne-particle abrasion, with larger alumina particles causing more severe changes. Aluminum traces on the 3Y-TZP surface are observed. The shape of the alumina particles is irregular, with rough edges; the size of the alumina particles plays a significant role in the air abrasion of zirconia-based dental ceramics, affecting their morphology and properties.

Keywords: zirconia; 3Y-TZP; airborne-particle abrasion; alumina; particle size

check for updates

Citation: Łagodzińska, P.; Dejak, B.; Konieczny, B. The Influence of Alumina Airborne-Particle Abrasion on the Properties of Zirconia-Based Dental Ceramics (3Y-TZP). *Coatings* **2023**, *13*, 1691. https://doi.org/10.3390/coatings13101691

Academic Editor: Günter Motz

Received: 29 August 2023
Revised: 17 September 2023
Accepted: 20 September 2023
Published: 26 September 2023

Copyright: © 2023 by the authors. Licensee MDPI, Basel, Switzerland. This article is an open access article distributed under the terms and conditions of the Creative Commons Attribution (CC BY) license (https://creativecommons.org/licenses/by/4.0/).

1. Introduction

High-strength ceramics have successfully been used in dental prosthetics as an alternative to metal alloys, particularly for single-crown and bridge frameworks and post- and core manufacturing. One such material commonly used in Dentistry is the zirconia-based ceramic 3Y-TZP (3 mol% yttria-stabilized tetragonal zirconia polycrystals). Indications for 3Y-TZP restorations also include monolithic crowns, implant abutments, and bridges in anterior and posterior dental arch areas [1–3]. Zirconia-based dental ceramics are esthetic and biocompatible and have no carcinogenic or mutagenic effects on human tissues [4]. They demonstrate superior mechanical properties to other types of ceramics. In particular, 3Y-TZP has a flexural strength of 1200 MPa, compressive strength of 2000 MPa, modulus of elasticity of 210 GPa, coefficient of thermal expansion of 10.5 $\times$ 10^{-6}/°C, density of >6 g/cm^3, porosity of <0.1, thermal conductivity of 2 W/mK, hardness of 1200 HV 0.1, and fracture toughness (KIc) of 10 MPa/m [5,6].

Although zirconia-based dental ceramics have outstanding mechanical properties, they suffer from weak bonding strength to veneering ceramics and resin cements. For example, 3Y-TZP is chemically inert and composed of densely packed crystals without a glass matrix [7]. However, the bond strength of 3Y-TZP with resin cements can be improved by various surface treatment methods. These include mechanical surface pretreatments, such as alumina airborne-particle abrasion, selective infiltration etching, laser pretreatment,

and tribochemical silica coating, and chemical surface treatments, such as phosphate, carboxylic primers, silanization, and acid etching solutions; in addition, chemo-mechanical surface treatments, i.e., combinations of the above methods, can be used, as well as recently introduced alternative methods [7].

Currently, the treatment of choice is alumina airborne-particle abrasion combined with the use of primers incorporating the 10-MDP monomer (10-methacryloyloxydecyl dihydrogen phosphate) [8–12]. The procedure has been found to significantly improve the bonding strength of zirconia-based dental restorations to resin cements [8,12–16] and to offer durable, long-term efficacy [16,17]. Moreover, alumina-particle air abrasion activates the surface of zirconia, increases its wettability, ensures micromechanical retention, and cleans the zirconia surface of organic and inorganic compound contamination [18]. Also, the procedure has been found to increase the biaxial flexural strength of zirconia-based dental ceramics [19–21]. On the other hand, alumina airborne-particle abrasion causes defects in the topmost layer of zirconia, such as micro-cracks, martensitic plate formation, irregular grooves, and fissures [22–26], and results in the embedding of alumina particles in the surface [25,27]. It also induces the tetragonal-to-monoclinic phase transformation, associated with phase transformation toughening (PTT) and low-temperature degradation (LTD). PTT is associated with an immediate increase in mechanical strength, while LTD is associated with material degradation and a gradual reduction in mechanical properties [6,28–30]. Recent studies have found that while alumina airborne-particle abrasion induces the tetragonal-to-monoclinic phase transformation, it does not affect the stability and reliability of restorations made of 3Y-TZP over time [21,31].

The effect of air abrasion on the extent of the changes made to the superficial layers of zirconia-based ceramics depends on various treatment conditions, such as the size of the alumina particles and the pressure of air abrasion [22,23,25,32–36]. They are believed to play a role in the surface morphology and roughness of abraded zirconia and the t-m transformation [23,25,32–34]. Alumina particle size has also been found to influence the surface hardness of 3Y-TZP [37,38]. Alumina-particle air abrasion can create a 10 μm degradation zone within the superficial layer [23]. The depth of the phase transformation induced by air abrasion is also influenced by the pressure of the treatment and the size of the alumina particles and may be detected at a depth ranging from 2.9 μm to 47.2 ± 3.0 μm of the zirconia surface [23,35,36]. The monoclinic volume may reach 3.99%–15.2% [19,20,22–26,33,34,39,40].

Studies indicate that while alumina airborne-particle abrasion can improve the bonding strength of 3Y-TZP to resin cements, it also affects its mechanical properties and the structure of the topmost layer of zirconia [8–16,19–21,23,25,32–36,41]. Although such changes following alumina air abrasion have already been reported, it is difficult to obtain a coherent understanding of the data, especially since many studies were not intended as specific assessments of the role of the size of the alumina particles used in air abrasion. No studies have assessed the effect of alumina particle size on the hardness of 3Y-TZP. In addition, surface roughness evaluations have usually only been based on Ra parameter assessment; this should be supplemented with microscope studies and SEM-EDS (scanning electron microscopy–energy-dispersive X-ray spectroscopy) examination to determine the degree of airborne-particle abrasion [42,43]. Therefore, to better understand the effects of treatment, a more thorough assessment of the additional properties of the 3Y-TZP surface, such as hardness, is required, together with a more precise determination of the roughness parameters, morphology, and elemental composition of the surface following air abrasion with different sizes of alumina particles.

Therefore, the aim of this study was to evaluate the effect of airborne-particle abrasion with three different sizes of alumina particles on the hardness of 3Y-TZP and to determine the effect on its roughness, structure, and elemental composition. The null hypothesis assumed that the use of different sizes of alumina particles for airborne-particle abrasion would not affect the hardness and roughness of the surface of zirconia-based dental ceramics, and that the surface morphology and elemental composition of the topmost surface of abraded zirconia would not change.

2. Materials and Methods

2.1. Specimen Preparation

Semi-circular blanks of commercial pre-sintered 3Y-TZP ceramics were used (Ceramill Zi; Amann Girrbach AG, Koblach, Austria). The technical data and chemical composition of the Ceramill Zi provided by the manufacturer are presented in Tables 1 and 2.

Table 1. Technical data of 3Y-TZP ceramics (Ceramill Zi; Amann Girrbach AG, Koblach, Austria) provided by the manufacturer.

Technical Data of 3Y-TZP		
	Unit	**Value**
Bending strength (4-point)	MPa	>1200
E-module	GPa	>200
Grain size	µm	≤0.6
Density	g/cm^3	≥6.07
Open porosity	%	0
Thermal expansion coefficient (WAK) (25–500 °C)	1/K	$10.0 \pm 0.5 \times 10^{-6}$
Chemical solubility	$\mu g/cm^2$	<5
Radioactivity	Bq/g	0.0156

Table 2. Chemical composition of 3Y-TZP (Ceramill Zi; Amann Girrbach AG, Koblach, Austria) provided by the manufacturer.

Chemical Composition of 3Y-TZP	
Oxide	**Mass Percentage**
$ZrO_2 + HfO_2 + Y_2O_3$	>99.0
Y_2O_3	4.5–5.6
HfO_2	<5
Al_2O_3	<0.5
Other oxides	<0.5

The surfaces of the specimens were subjected to Vickers hardness evaluation, zirconia roughness evaluation, and SEM–EDS microanalysis following airborne-particle abrasion with alumina particles of three sizes: 50 µm, 110 µm, and 250 µm.

Cuboid-shaped zirconia-based samples measuring 5 × 5 × 20 mm were designed (assuming 21% material shrinkage, as indicated by the manufacturer) and processed using a Ceramill Mind milling machine (Amann Girrbach AG, Koblach, Austria). The specimen design was converted to milling strips and loaded into the milling machine, where it was dry-processed (Ceramill Motion; Amann Girrbach AG, Koblach, Austria). The milled specimens were then sintered in the furnace for 10 h (Ceramill Therm; Amann Girrbach AG, Koblach, Austria) with the temperature rising from 200 °C to 1450 °C (8 °C/min), after which the temperature was kept constant at 1450 °C for two hours, and then the samples were allowed to gradually cool. The dimensions of the final specimens were 4 × 4 × 15.8 mm.

The cuboid specimens were randomly divided into four groups. In one group, the surfaces of the specimens were left untreated (control group): the surface was only mechanically processed during the milling procedure, preceding the sintering process. Such surfaces are obtained during the clinical preparation of prosthetic restorations and can be left as is or later modified before the application of cements. In the three other groups, the specimens were air-abraded with alumina particles either 50 µm, 110 µm, or 250 µm in size, depending on the group (Alustral; Omnident Dental Handelsgesellschaft mbH, Rodgau, Germany). The conditions of air abrasion were equal for all the specimens: 45° angle, 13 mm distance, pressure of 3 bars, and 10 s (Basic Classic Renfert GmbH, Hilzingen, Germany).

2.2. The Vickers Hardness Evaluation of 3Y-TZP

The hardness of zirconia after airborne-particle abrasion with three sizes of alumina particles was determined using the Vickers indentation method. Thirteen measurements were recorded for each group (the group division is described above). The Zwick Roell Indentec hardness tester was used (Zwick/Roell ZHμ; Zwick Roell Indentec; Zwick GmbH & Co. KG, Ulm, Germany). A diamond-pyramid-shaped indenter was pressed into a specimen firmly supported on the metal base. The tested load was HV 1, applied for 15 s, and perpendicular to the tested surface. Following this, the indentation diameter length was measured, and the value of Vickers hardness was calculated.

2.3. The Zirconia Roughness Evaluation

The surface roughness of the specimens was tested before and after air abrasion with alumina particles using a profilometer (Portable Surface Roughness Tester SURFTEST SJ-410 Series; Mitutoyo America Corporation, Aurora, CO, USA). Measurements were made for each sample along the measurement length. The values of Ra, Rq, Rz, Rsk, Rsm, Rt, and Vo were assessed, and the profile displays were recorded (Table 3).

Table 3. The description of the surface roughness parameters.

Surface Roughness Parameter	Description
Ra	Roughness average: arithmetic mean deviation of the roughness profile; the arithmetic mean value of the absolute deviations of the profile from the mean line. This value is related to abrasive wear.
Rq	RMS roughness: root-mean-square deviation of the profile.
Rz	Average maximum height of the profile: roughness profile height according to 10 points: this is the mean of the height of the five highest profile points above the mean line, reduced by the height of the five lowest profile points.
Rsk	Skewness: a measure of the asymmetry of the profile to the mean line; a negative value indicates that a greater percentage of the profile is below the mean line, while a positive value indicates that more of the profile is above the line.
Rsm	Mean spacing of profile irregularities: the mean width of the profile elements; the mean value of the roughness intervals.
Rt	Maximum height of the roughness profile: the vertical distance measured between the highest and the lowest points of the profile.
Vo	Retention volume: the area in a roughness profile measured between the ratio curve and the one-hundred-percent material line below the core roughness.

2.4. SEM–EDS Microanalysis

The microstructures of the surfaces of all specimens (untreated controls and the three groups subjected to air abrasion) were assessed with an electron microscope at 2500× magnification (S-4700 scanning electron microscope; Hitachi High-Technologies Corporation, Tokyo, Japan). Prior to SEM analysis, the surface of each specimen was covered with a thin layer of carbon (The Cressington 108carbon/A; Cressington Scientific Instruments Ltd., Watford, UK).

The energy-dispersive X-ray microanalysis was performed with an EDS detector (Ultra-Dry Silicon drift X-ray detector; Thermo Electron Scientific Instruments LLC, Madison, MA, USA) to determine the elemental compositions of the topmost layers of zirconia specimens before and after air abrasion with alumina particles of three sizes. The images were acquired with an electron microscope at a magnification of 5000× (Scanning Electron Microscope S-4700; Hitachi High-Technologies Corporation, Tokyo, Japan). The accelerating voltage was set to 25.0 kV.

An additional assessment included acquiring images of 50 μm, 110 μm, and 250 μm alumina particles at 250× magnification with the S-4700 scanning electron microscope (Hitachi High-Technologies Corporation, Tokyo, Japan).

2.5. Statistical Analysis

The results were compared using the Kruskal–Wallis one-way analysis-of-variance-by-ranks test, a nonparametric analog of the one-way analysis of variance. p values < 0.05 were considered statistically significant.

3. Results

The results obtained in the Vickers hardness test are shown in Figure 1. It was found that only the group subjected to 50 µm alumina-particle air abrasion (1678.8 HV1kp) demonstrated any significant difference in hardness after treatment ($p < 0.001$; Kruskal–Wallis one-way ANOVA). No significant differences ($p = 0.05$) were found between untreated controls (1545.2 HV1kp) and the groups treated with 110 µm particles (1525.5 HV1kp) and 250 µm particles (1515.4 HV1kp).

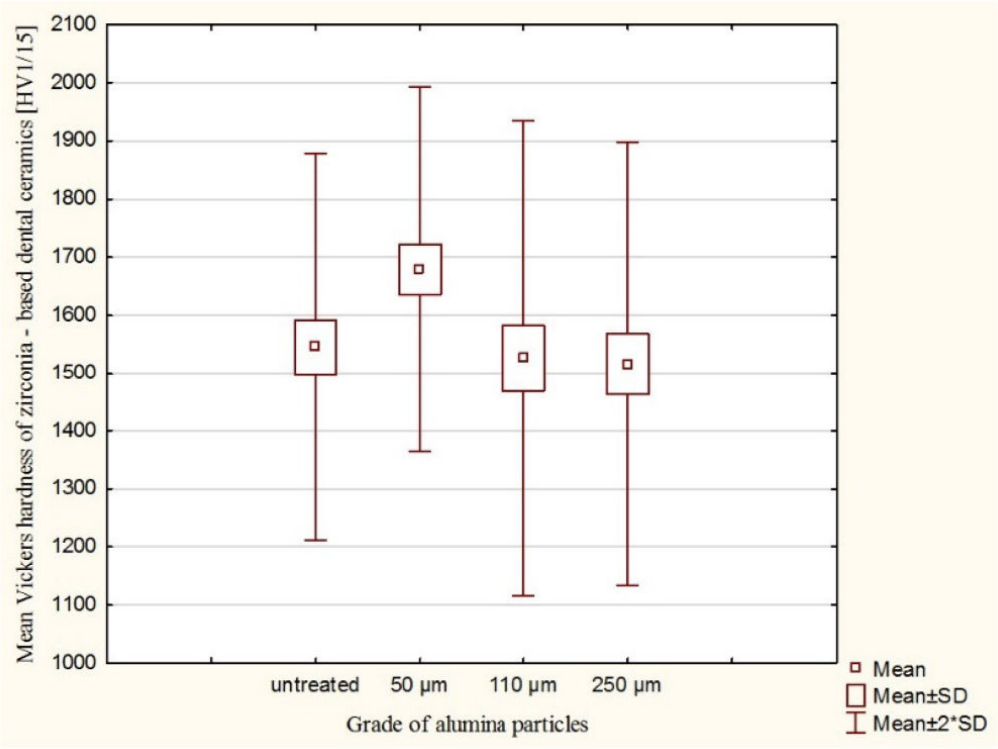


Figure 1. The Vickers hardness of zirconia-based dental ceramics. The figure presents the mean values (HV1kp) of all tested groups: untreated specimens (1545.2 HV1kp) and those air-abraded with alumina particles of 50 µm (1678.8 HV1kp), 110 µm (1525.5 HV1kp), or 250 µm (1515.4 HV1kp).

The surface roughness evaluation provided a quantitative analysis of the surface profile geometry in the four groups. The mean values of the surface roughness parameters are shown in Table 4, and the profile displays for each group are given in Figure 2. The values of Ra, Rq, Rz, Rt, and Vo increased with the size of alumina particles used for air abrasion. A higher Rsm was noted for specimens air-abraded with 250 µm alumina particles. The surface roughness profile of zirconia specimens abraded with 50 µm alumina particles was symmetrical (Rsk).

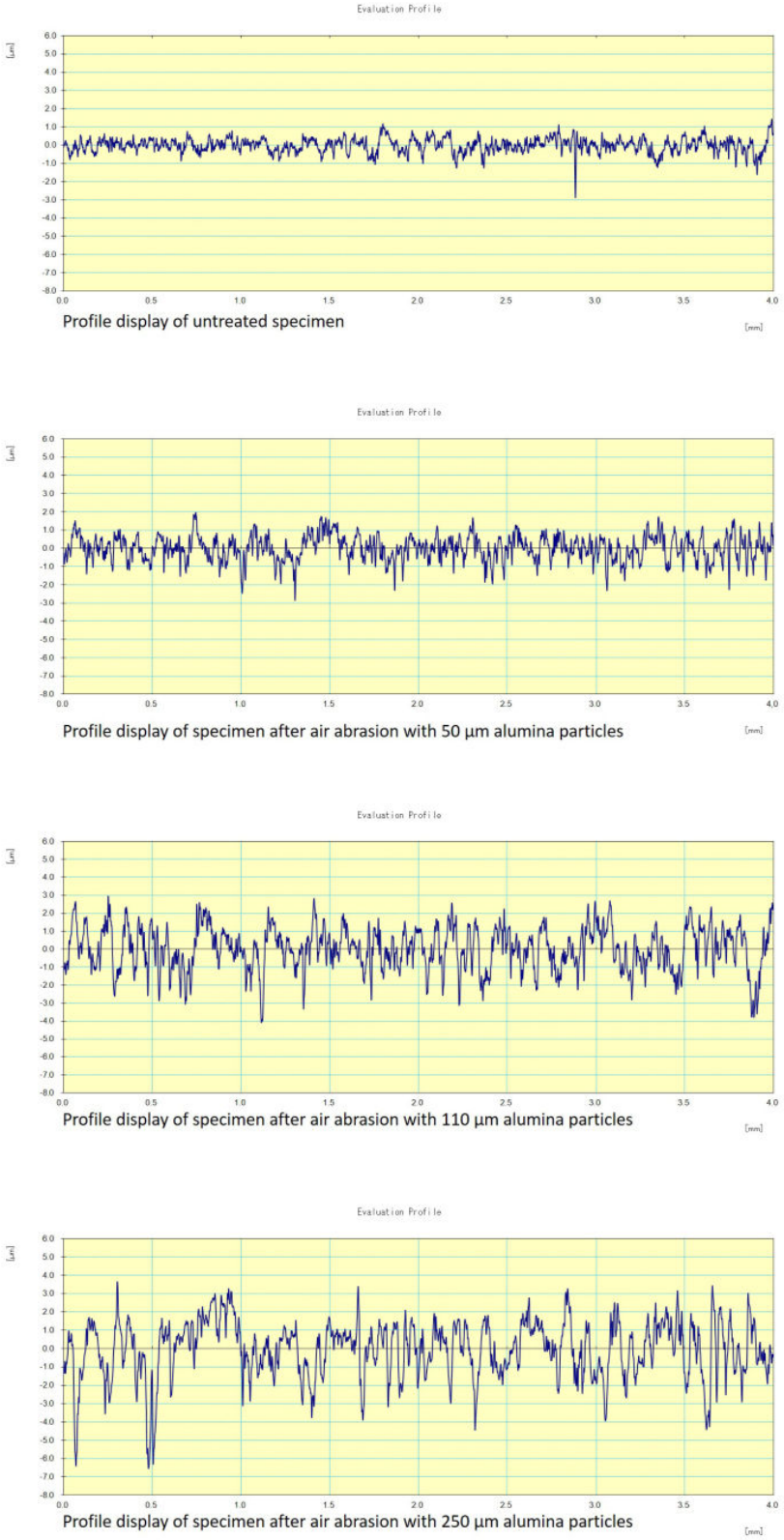


Figure 2. Profile displays demonstrating differences in the surface roughness between the tested groups: specimens with untreated surface and specimens air-abraded with alumina particles of 50 µm, 110 µm, or 250 µm. The profilograms represent the surface characterization within the evaluation length (the profile peaks and valleys), obtained with a moving stylus.

Table 4. The mean values of the profile surface roughness parameters in tested groups: specimens with untreated surface and specimens air-abraded with alumina particles of various sizes: 50 µm, 110 µm, 250 µm.

Researched Groups (Size of Alumina Particles Used For Air Abrasion)	Surface Roughness Parameters						
	Ra (µm)	Rq (µm)	Rz (µm)	Rsk	Rsm (µm)	Rt (µm)	Vo ($\mu m^3/\mu m^2$)
Untreated	0.286	0.383	3.053	0.218	161.300	5.133	0.003
50 µm	0.668	0.838	5.106	−0.001	132.233	6.400	0.006
110 µm	0.909	1.139	6.989	−0.233	116.833	8.264	0.007
250 µm	1.501	1.882	13.773	−0.131	304.300	13.773	0.010
P	0.0156	0.0156	0.0156	0.0987	0.0572	0.0188	0.0156

The SEM analysis provided a qualitative assessment of the zirconia surface geometry in the three treated groups and the untreated controls (Figure 3). The SEM analysis showed that the major topographic pattern differentiation changed with the size of alumina particles. Treatment with larger alumina particles was associated with more severe changes, such as irregularities, micro-cracks, grooves, and melted areas.

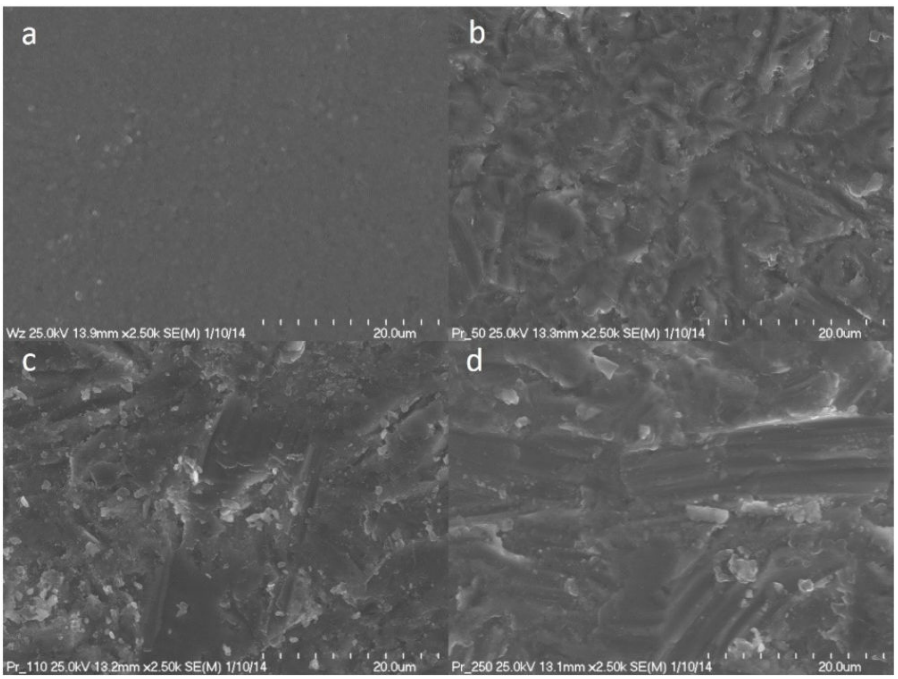


Figure 3. SEM micrographs of zirconia specimen surfaces at magnification 2500× for all tested groups: (**a**) untreated specimens with specimens treated with alumina particles of (**b**) 50 µm, (**c**) 110 µm, and (**d**) 250 µm.

Representative micrographs of the elemental distribution maps are presented in Figures 4–7. Sandblasting zirconia with alumina particles left aluminum traces on the zirconia surface, irrespective of the alumina particle size; these traces represented contamination caused by alumina-particle air abrasion. However, aluminum traces were also detected on the zirconia surface in the control group; this was related to the chemical composition of 3Y-TZP (Al_2O_3 < 0.5%), as presented in Table 2. The aluminum traces detected on the untreated surface were regularly distributed, while those found on the treated specimens were clearly visible and demarcated (Figures 5–7).

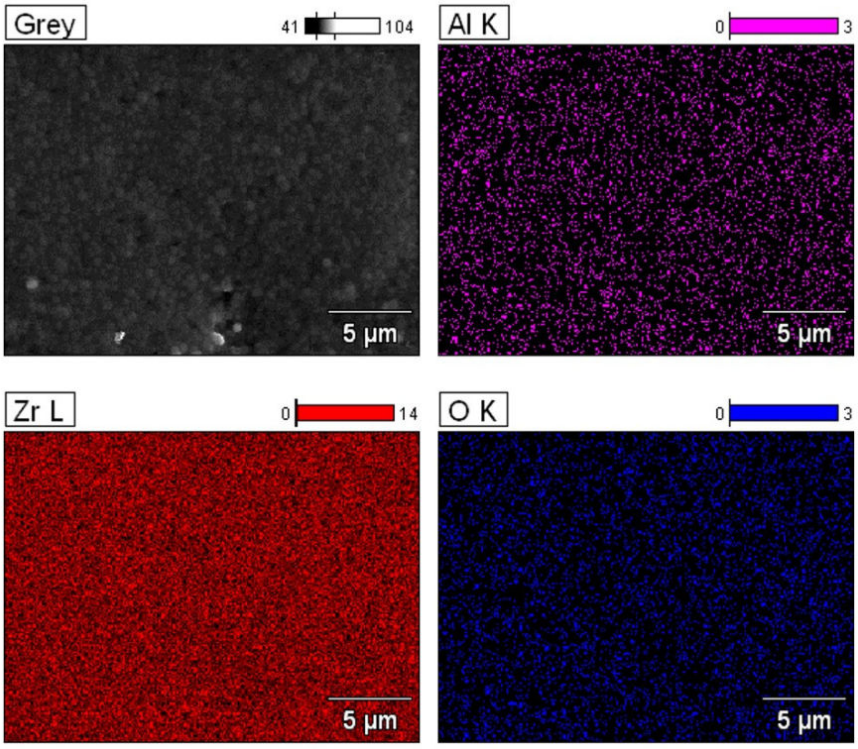


Figure 4. The elemental distribution maps of untreated zirconia surface (O—oxygen; Zr—zirconium; Al—aluminum).

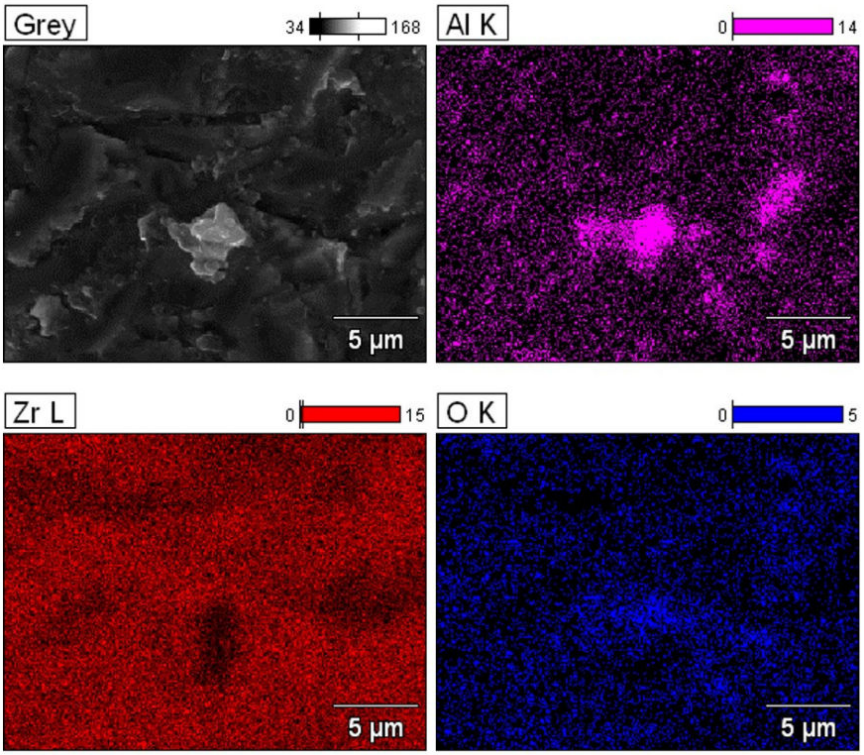


Figure 5. The elemental distribution maps of zirconia surface after airborne-particle abrasion with 50 µm alumina particles (O—oxygen; Zr—zirconium; Al—aluminum).

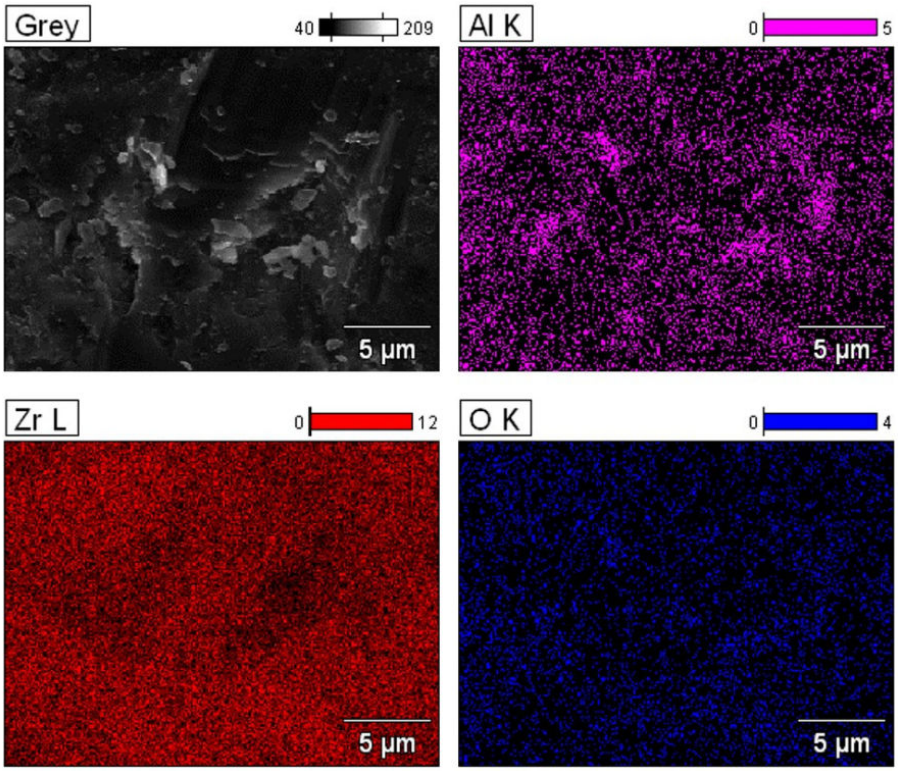


Figure 6. The elemental distribution maps of zirconia surface after airborne-particle abrasion with 110 µm alumina particles (O—oxygen; Zr—zirconium; Al—aluminum).

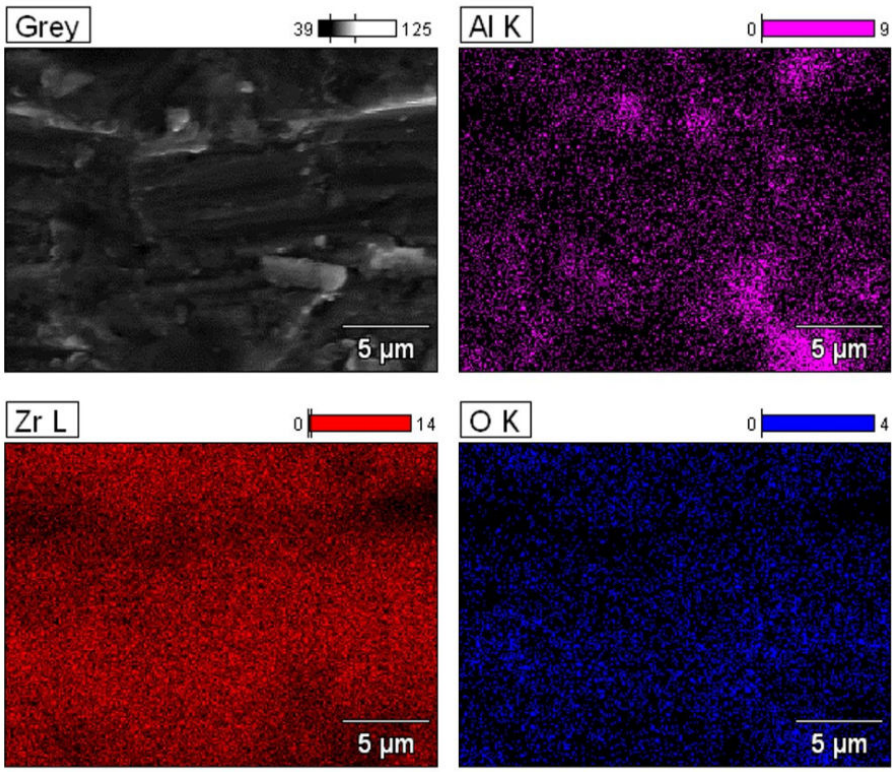


Figure 7. The elemental distribution maps of zirconia surface after airborne-particle abrasion with 250 µm alumina particles (O—oxygen; Zr—zirconium; Al—aluminum).

The SEM images of the initial analysis of the shape of alumina particles (50 μm, 110 μm, 250 μm) are presented in Figure 8. The shape of alumina particles was irregular with rough edges. As their shape is not spherical as expected, this may affect the degradation pattern present on the zirconia surface after air abrasion.

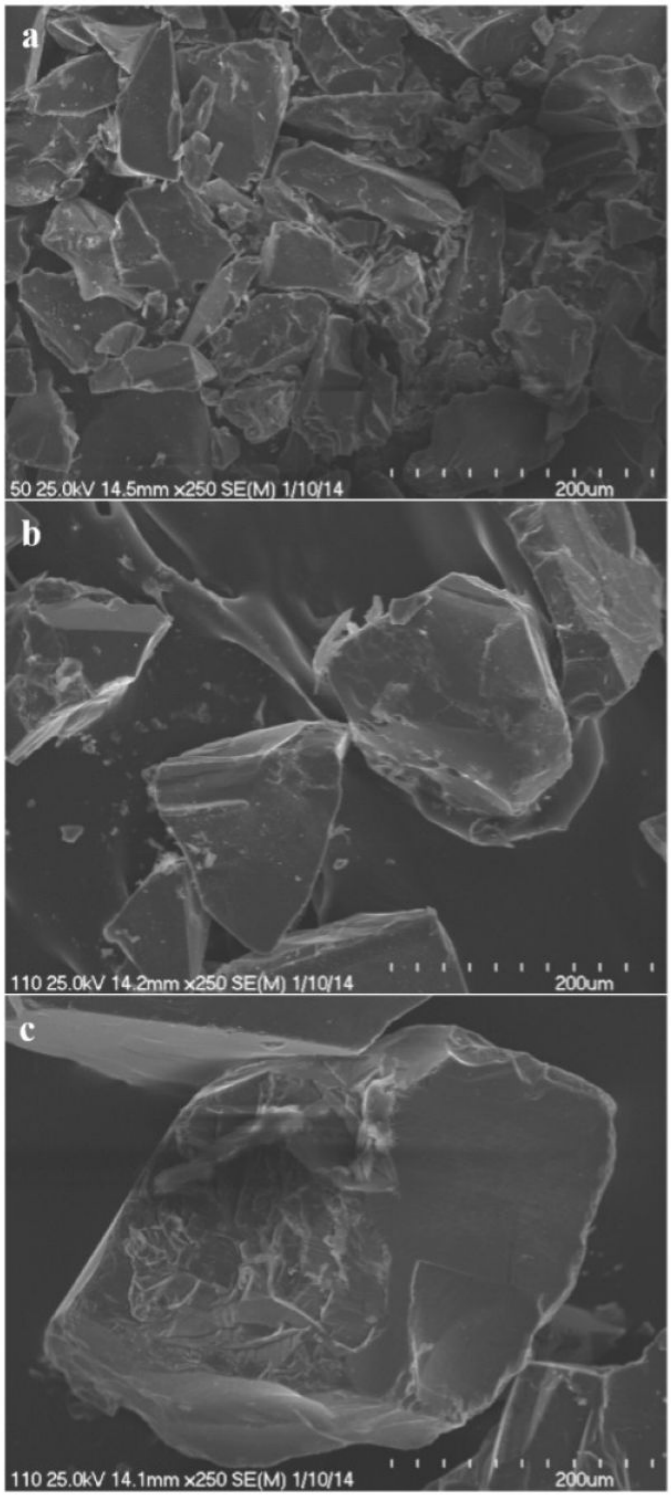


Figure 8. The SEM micrograph of alumina particles of different sizes: (**a**) 50 μm Al_2O_3, (**b**) 110 μm Al_2O_3, (**c**) 250 μm Al_2O_3 (250× magnification).

4. Discussion

The aim of this study was to determine the influence of alumina particle size on the properties of 3Y-TZP subjected to air abrasion based on a comparison of three different sizes. The material hardness, roughness, surface microstructure, topography, and elemental composition were assessed.

The hardness of a material is defined as its resistance to irreversible plastic deformation induced by localized mechanical indentation. Our findings indicate that the hardness of zirconia-based dental ceramics was significantly increased when its surface was treated with 50 µm alumina particles (1678.8 HV1KP). In contrast, air abrasion with 110 µm or 250 µm alumina particles did not influence the hardness, with the treated specimens demonstrating similar hardness to that of untreated specimens. Similar conclusions were reached by Shishido et al., who measured the Vickers hardness of 3Y-TZP after 50 µm alumina air abrasion [37]. Chintapalli et al. compared the hardness of zirconia specimens air-abraded with 110 µm alumina particles (at a pressure of 2 bar) with untreated specimens (16.0 GPa vs. 17.0 GPa). They found no significant differences between the two groups and concluded that the additional air abrasion with 110 µm alumina particles does not influence the zirconia hardness [38]. Such a result is consistent with our present findings.

A study of the influence of grinding the zirconia surface with different grain size burs (Mani Dia diamond bur standard grit, Tri Hawk diamond bur coarse grit, and Predator carbide bur) by Sandhu et al. found the coarseness of the dental bur to have no significant effect on the zirconia hardness. Moreover, the hardness of zirconia was significantly decreased by grinding [44]. Traini et al. found the coarse or fine polishing of a zirconia surface to have no significant influence on its hardness compared with the untreated surface [45]. Maerten et al. demonstrated that the mechanical treatment of a zirconia surface significantly decreases its hardness; the study compared untreated zirconia specimens with those that were polished with diamond discs and polish paste and those that were polished with diamond discs and polish paste and sintered again [46]. Resintering restored the untreated material's hardness [46]. Hence, it appears that grinding with burs is a more aggressive treatment than air abrasion and creates a rougher surface, that grinding decreased the hardness of zirconia [38,44–46], and that the coarseness of burs had no significant influence [44,45]. In the current study, only air abrasion with 50 µm alumina particles increased the hardness of zirconia, which may be explained by the phenomenon of phase transformation toughening. However, it needs to be emphasized that excessive surface roughness may interfere with hardness measurements [38]. Indeed, Shishido et al. indicate that Vickers hardness assessment is a more reliable approach to testing smooth specimen surfaces and that excessive roughness decreases precision when measuring diagonals [37].

The surface morphology of 3Y-TZP treated with air abrasion has been assessed by surface roughness evaluation and SEM observations. In the current study, seven roughness parameters (Table 3) were used to comprehensively analyze the surface roughness (horizontal and vertical planes, skewness, retention volume). The profile heights were assessed using a number of commonly used parameters: Ra, Rq (the average of profile heights), Rz (the mean of the profile heights and depths), and Rt (the distance between the highest and lowest profile points, vertical). These parameters increased with the size of alumina particles used for air abrasion.

The horizontal plane, i.e., the mean spacing between the irregularities of the profile, was assessed with Rsm. Broader profile irregularities were associated with 250 µm alumina-particle air abrasion. The skewness of the profile was assessed using Rsk, indicating profile asymmetry. The profile of the zirconia surface was found to be symmetrical for 50 µm particle air abrasion but above the mean line for 110 and 250 µm particles. The retention volume (Vo) increased with the increase in the alumina particle size used for air abrasion.

Our findings indicate that air abrasion with alumina particles creates a rough and irregular surface with micro-retentive grooves that may enhance the bond strength of 3Y-TZP to resin cements. Such treatment not only extends the bonding surface but also

increases the wettability and interfacial free energy of zirconia [9]. Air abrasion with larger alumina particles leads to an increase in surface roughness in both the vertical and horizontal planes, as well as in retention volume. The most predictable and mild effects were obtained after air abrasion with 50 μm alumina particles, as this created a symmetrical profile with less severe irregularities than after treatment with 110 μm and 250 μm alumina particles. Air abrasion with larger alumina particles may decrease the bonding capacity of zirconia to resin cements. These findings are supported by those of previous studies [12]. The wider and deeper grooves that are formed may prevent the proper filling of the profile valleys with resin agents and cause air bubble entrapment. Our present findings are supported by those of other authors; however, previous studies have mainly evaluated Ra surface roughness. Nevertheless, they proved that the 3Y-TZP surface roughness increased with the size of alumina particles used for air abrasion and confirmed a significant increase when compared to untreated specimens [23,26,33,35,39,40,47,48].

Our surface roughness assessment is supported by our present SEM observations. The microstructure of the topmost layer of air-abraded zirconia was distinctly changed when compared to the untreated specimens. As can be seen in the SEM images (Figure 3), the treated surface is pitted with fissures, cracks, and irregular grooves, which increase in severity with the size of the alumina particles. Similar observations have been made in previous studies also indicating that airborne alumina abrasion creates rough zirconia surfaces with alterations [19,22–26,32–35,47]. Regarding the effect of particle size, Hallmann et al. found that a larger size resulted in greater degradation of the zirconia surface [34]. Chintapalli et al. also indicated that air abrasion with larger particles increases the damage to the zirconia surface and results in the presence of larger cracks and gaps; a cross-section SEM analysis showed a crystal-deformation zone within 2–3 μm of the topmost zirconia layer, as well as micro-cracks and martensite plate formation described as monoclinic phase clusters [23].

Our present findings confirm the presence of alumina particles on the surfaces of both the treated 3Y-TZP samples and the untreated specimens; however, their content was lower in the latter and can be easily explained by the composition of the 3Y-TZP blocks, i.e., $ZrO_2 + HfO_2 + Y_2O_3 > 99\%$, where Y_2O_3~4.5%–5.6%, $HfO_2 < 5\%$, $Al_2O_3 < 0.5\%$, and other oxides < 0.5% (manufacturer's data) [Table 2]. Hallmann et al. also report the presence of aluminum traces on the zirconia surface after air abrasion, together with an increase in aluminum content from 0.25% to 2.85%. They also indicate that alumina particles used for air abrasion are sharp, and their shapes are irregular [25].

Elsewhere, Hallmann et al. also found that the air abrasion of zirconia with 110 μm alumina particles at a pressure of 3.5 bar resulted in a 5.4% composition of aluminum on the surface. Looser deposits of alumina were observed at lower pressures, while the alumina particles became embedded into the zirconia surface at higher pressure [34]. By calculating the aspect ratio of the longest to the shortest diameter of a particle, they also found the 50 μm alumina particles to be sharper than the 110 μm alumina particles and that this shape can affect the damage characteristics [34]. They propose that such looser adherence may reduce the bonding strength of zirconia to resin cements [34].

Śmielak et al. report that alumina particle size significantly affects the aluminum content detected on the zirconia surface after air abrasion. Treatment with 110 μm and 250 μm alumina particles resulted in 4.51%–4.99% aluminum on the surface, while treatment with 60 μm particles resulted in 6.085%. A significantly higher share of aluminum was detected for abrasion with 60 μm particles than for the larger particles [27].

Although airborne-particle abrasion with alumina particles leaves deposits of the abrasive on the zirconia surface, it is still an effective method for removing organic and inorganic contamination. Quass et al. found alumina airborne-particle abrasion to be the most effective method of removing organic contaminants (i.e., saliva) from the zirconia surface, while alcohol application or 37% orthophosphoric acid etching was not as efficient [18].

Taken together, our present findings indicate that airborne alumina-particle abrasion roughens the zirconia surface, creates micro-retentive grooves, and leaves alumina

particle deposits on the zirconia surface. It mildly affects the zirconia hardness. The apparent benefits of alumina air abrasion are a significant increase in the bond strength of zirconia to resin cements and the efficient cleaning of the zirconia surface by removing contaminants [8,13–16,18]. Many researchers have found that such treatment results in an increase in the monoclinic phase content within the topmost layer of zirconia [23,25,33,34,41] while also increasing the biaxial flexural strength of zirconia [19–21]. Airborne-particle abrasion affects the microstructure of the superficial surface of zirconia by creating irregular grooves, which are considered a degradation zone [23,25,33,34]. Recent studies, however, indicate that airborne-particle abrasion with alumina particles may not affect the stability of zirconia ceramic, and it can even enhance its resistance to LTD compared to untreated 3Y-TZP [21,31]. Hence, airborne alumina-particle abrasion appears to be a favorable treatment for the surface of zirconia before adhesive cementation; however, the parameters of air abrasion should be carefully adjusted.

Our findings have various clinical implications, most importantly that the use of smaller alumina particles in the air abrasion of zirconia-based dental ceramics yields the least negative effect on the zirconia microstructure while still roughening the surface before adhesive cementation.

Limitation of the study: This study is a laboratory assessment of the influence of alumina airborne-particle abrasion with different sizes of alumina particles on the surfaces of zirconia-based dental ceramics. It did not take into account the aging processes of zirconia-based dental ceramics and the clinical behavior of this material. In addition, while the results indicate that the size of alumina particles can influence the microhardness, roughness, and surface topography of 3Y-TZP, the assessment did not include 4Y-TZP or 5Y-TZP ceramics. Also, the material hardness could not be as accurately determined on rough surfaces due to the need to obtain precise measurements of the diagonals of the indentations. In the end, the characterization of alumina particles performed herein should be regarded as an initial analysis.

5. Conclusions

The properties of the zirconia-based dental ceramic 3Y-TZP are affected by airborne-particle abrasion, and the size of the alumina particles has a significant influence on the results. Our findings indicate that air abrasion with 50 μm alumina particles resulted in a significantly higher Vickers hardness of zirconia-based dental ceramics, while no such increase was observed for larger alumina particles. In addition, alumina-particle air abrasion also influenced the roughness and topography of the samples, with micro-cracks and irregular grooves being observed. The surface roughness was found to increase with alumina particle size. The intensity of zirconia surface alterations also increased with alumina particle size. Air abrasion results in alumina particles being embedded in the topmost surface of zirconia. The shape of the alumina particles is irregular and sharp.

Author Contributions: Conceptualization, P.Ł. and B.D.; Methodology, P.Ł., B.D. and B.K.; Software, B.K.; Validation, P.Ł. and B.D.; Formal analysis, P.Ł. and B.D.; Investigation, P.Ł.; Resources, P.Ł., B.D. and B.K.; Writing—original draft, P.Ł.; Writing—review & editing, B.D. and B.K.; Visualization, P.Ł.; Supervision, B.D.; Funding acquisition, B.D. All authors have read and agreed to the published version of the manuscript.

Funding: This research was supported through a grant 502-03/2-148-03/502-24-005 provided by the Medical University of Lodz to Paulina Łagodzińska and Prof. Beata Dejak. The research was conducted in the University Material Testing Laboratory, Lab Head Prof. Jerzy Sokołowski.

Institutional Review Board Statement: Not applicable.

Informed Consent Statement: Not applicable.

Data Availability Statement: Not applicable.

Conflicts of Interest: The authors declare no conflict of interest.

References

1. Gamborena, I.; Blatz, M.B. A clinical guidelines to predictable esthetics with zirconium oxide ceramic restorations. *Quintessence Dent. Technol.* **2006**, *29*, 11–23.
2. Potiket, N.; Chiche, G.; Finger, I.M. In vitro fracture strength of teeth restored with different all-ceramic crown systems. *J. Prosthet. Dent.* **2004**, *92*, 491–495. [CrossRef] [PubMed]
3. Larsson, C.; Vult von Steyern, P.; Sunzel, B.; Nilner, K. Allceramic two- to five-unit implant-supported reconstructions. A randomized, prospective clinical trial. *Swed. Dent. J.* **2006**, *30*, 45–53. [PubMed]
4. Covacci, V.; Bruzzese, N.; Maccauro, G.; Andreassi, C.; Ricci, G.A.; Piconi, C.; Marmo, E.; Burger, W.; Cittadini, A. In vitro evaluation of the mutagenic and carcinogenic power of high purity zirconia ceramic. *Biomaterials* **1999**, *20*, 371–376. [CrossRef] [PubMed]
5. Piconi, C.; Maccauro, G. Zirconia as a ceramic biomaterial. *Biomaterials* **1999**, *20*, 1–25. [CrossRef] [PubMed]
6. Sakaguchi, R.L.; Powers, J.M. *Craig's Restorative Dental Materials*; Elsevier Ltd.: Oxford, UK, 2011; pp. 253–285.
7. Khan, A.A.; Al Kheraif, A.A.; Jamaluddin, S.; Elsharawy, M.; Divakar, D.D. Recent Trends in Surface Treatment Methods for Bonding Composite Cement to Zirconia: A Review. *J. Adhes. Dent.* **2017**, *19*, 7–19. [PubMed]
8. Blatz, M.B.; Phark, J.-H.; Ozer, F.; Mante, F.K.; Saleh, N.; Bergler, M.; Sadan, A. In vitro comparative bond strength of contemporary self-adhesive resin cements to zirconium oxide ceramic with and without air-particle abrasion. *Clin. Oral Investig.* **2010**, *14*, 187–192. [CrossRef] [PubMed]
9. Blatz, M.B.; Sadan, A.; Martin, J.; Lang, B. In vitro evaluation of shear bond strengths of resin to densely sintered high-purity zirconium-oxide ceramic after long-term storage and thermal cycling. *J. Prosthet. Dent.* **2004**, *91*, 356–362. [CrossRef]
10. Yoshida, K.; Tsuo, Y.; Atsuta, M. Bonding of dual-cured resin cement to zirconia ceramic using phosphate acid estermonomer and zirconate coupler. *J. Biomed. Mater. Res. B Appl. Biomater.* **2006**, *77B*, 28–33. [CrossRef]
11. Blatz, M.B.; Chiche, G.; Holst, S.; Sadan, A. Influence of surface treatment and simulated aging on bond strengths of luting agents to zirconia. *Quintessence Int.* **2007**, *38*, 745–753.
12. Łagodzińska, P.; Bociong, K.; Sokołowski, J.; Dejak, B. Comparative study of the shear bond strength of zirconia-based dental ceramics to resin cements after chemo-mechanical surface modification. *J. Stoma* **2019**, *72*, 158–166. [CrossRef]
13. Gomes, A.L.; Castillo-Oyague, R.; Lynch, C.D.; Montero, J.; Albaladejo, A. Influence of sandblasting granulometry and resin cement composition on microtensile bond strength to zirconia ceramic for dental prosthetic framework. *J. Dent.* **2013**, *41*, 31–41. [CrossRef] [PubMed]
14. Phark, J.-H.; Duarte, S.; Blatz, M.; Sadan, A. An in vitro evaluation of the long-term resin bond to a new densely sintered high-purity zirconium-oxide ceramic surface. *J. Prosthet. Dent.* **2009**, *101*, 29–38. [CrossRef] [PubMed]
15. Yun, J.; Ha, S.; Lee, J.; Kim, S. Effect of sandblasting and various metal primers on the shear bond strength of resin cement to Y-TZP ceramic. *Dent. Mater.* **2010**, *26*, 650–658. [CrossRef] [PubMed]
16. Yang, B.; Barloi, A.; Kern, M. Influence of air–abrasion on zirconia ceramic bonding using an adhesive composite resin. *Dent. Mater.* **2010**, *26*, 44–50. [CrossRef] [PubMed]
17. Tsuo, Y.; Yoshida, K.; Atsuta, M. Effects of alumina-blasting and adhesive primers on bonding between resin luting agent and zirconia ceramics. *Dent. Mater. J.* **2006**, *25*, 669–674. [CrossRef] [PubMed]
18. Quaas, A.C.; Yang, B.; Kern, M. Panavia F 2.0 bonding to contaminated zirconia ceramic after different cleaning procedures. *Dent. Mater.* **2007**, *23*, 506–512. [CrossRef] [PubMed]
19. Kosmac, T.; Oblak, C.; Jevnikar, P.; Funduk, N.; Marion, L. Strength and reliability of surface treated Y-TZP dental ceramics. *J. Biomed. Mater. Res. B Appl. Biomater.* **2000**, *53*, 304–313. [CrossRef]
20. Kosmac, T.; Oblak, C.; Jevnikar, P.; Funduk, N.; Marion, L. The effect of Surface grinding and sandblasting on flexural strength and reliability of 3Y-TZP zirconia ceramic. *Dent. Mater.* **1999**, *15*, 426–433. [CrossRef]
21. Cotic, J.; Jevnikar, P.; Kocjan, A. Ageing kinetics and strength of airborne- particle abraded 3Y-TZP ceramics. *Dent. Mater.* **2017**, *33*, 847–856. [CrossRef]
22. Guazzato, M.; Quach, L.; Albakry, M.; Swain, M.V. Influence of surface and heat treatments on the flexural strength of Y-TZP dental ceramic. *J. Dent.* **2005**, *33*, 9–18. [CrossRef] [PubMed]
23. Chintapalli, R.K.; Marro, F.G.; Jimenez-Pique, E.; Anglada, M. Phase transformation and subsurface damage in 3Y-TZP after sandblasting. *Dent. Mater.* **2013**, *29*, 566–572. [CrossRef] [PubMed]
24. Zhang, Y.; Lawn, B.R.; Rekow, E.D.; Thompson, V.P. Effect of sandblasting on the long term performance of dental ceramics. *J. Biomed. Mater. Res. B Appl. Biomater.* **2004**, *71B*, 381–386. [CrossRef] [PubMed]
25. Hallmann, L.; Ulmer, P.; Reusser, E.; Hammerle, C.F. Surface characterization of dental Y-TZP ceramic after air abrasion treatment. *J. Dent.* **2012**, *40*, 723–735. [CrossRef] [PubMed]
26. Sato, H.; Yamadad, K.; Pezzotti, G.; Nawa, M.; Ban, S. Mechanical properties of dental zirconia ceramics changed with sandblasting and heat treatment. *Dent. Mater. J.* **2008**, *27*, 408–414. [CrossRef] [PubMed]
27. Śmielak, B.; Klimek, L. Effect of air abrasion on the number of particles embedded in Zirconia. *Materials* **2018**, *11*, 259. [CrossRef] [PubMed]
28. Garvie, R.C.; Hannink, R.H.; Pascoe, R.T. Ceramic steel? *Nature* **1975**, *258*, 703–704. [CrossRef]
29. Lughi, V.; Sergo, V. Low temperature degradation–aging- of zirconia: A critical review of the relevant aspects in dentistry. *Dent. Mater.* **2010**, *26*, 807–820. [CrossRef]

30. Swab, J.J. Low temperature degradation of Y-TZP materials. *J. Mater. Sci.* **1991**, *26*, 6706–6714. [CrossRef]
31. Inokoshi, M.; Vanmeensel, K.; Zhang, F.; De Munck, J.; Eliades, G.; Minakuchi, S.; Naert, I.; Meerbeek, B.; Vleugels, J. Aging resistance of surface–treated dental zirconia. *Dent. Mater.* **2015**, *31*, 182–194. [CrossRef]
32. Kim, H.-K.; Ahn, B. Effect of Al_2O_3 Sandblasting Particle Size on the Surface Topography and Residual Compressive Stresses of Three Different Dental Zirconia Grades. *Materials* **2021**, *14*, 610. [CrossRef] [PubMed]
33. Monaco, C.; Tucci, A.; Esposito, L.; Scotti, R. Microstructural changes produced by abrading y-TZP in presintered and sintered conditions. *J. Dent.* **2013**, *41*, 121–126. [CrossRef] [PubMed]
34. Hallmann, L.; Ulmer, P.; Reusser, E.; Hammerle, C.F. Effect of blasting pressure, abrasive particle size and grade on phase transformation and morphological change of dental zirconia surface. *Surf. Coat. Technol.* **2012**, *206*, 4293–4302. [CrossRef]
35. Wongkamhaeng, K.; Dawson, D.V.; Holloway, J.A.; Denry, I. Effect of Surface Modification on In-Depth Transformations and Flexural Strength of Zirconia Ceramics. *J. Prosthodont.* **2019**, *28*, e364–e375. [CrossRef]
36. Kim, H.-K.; Yoo, K.-W.; Kim, S.-J.; Jung, C.-H. Phase Transformations and Subsurface Changes in Three Dental Zirconia Grades after Sandblasting with Various Al_2O_3 Particle Sizes. *Materials* **2021**, *14*, 5321. [CrossRef] [PubMed]
37. Shishido, S.; Inagaki, R.; Kanno, T.; Svanborg, P.; Barkarmo, S.; Ortengren, U.; Nakamura, K. Residual stress associated with crystalline phase transformation of 3–6 mol% yttria-stabilized zirconia ceramics induced by mechanical surface treatments. *J. Mech. Behav. Biomed. Mater.* **2023**, *146*, 106067. [CrossRef] [PubMed]
38. Chintapalli, R.K.; Rodriguez, A.M.; Marro, F.G.; Anglada, M. Effect of sandblasting and residual stress on strength of zirconia for restorative dentistry applications. *J. Mech. Behav. Biomed. Mater.* **2014**, *29*, 126–137. [CrossRef]
39. Karakoca, S.; Yilmaz, H. Influence of surface treatments on surface roughness, phase transformation, and biaxial flexural strength of 3Y-TZP ceramics. *J. Biomed. Mater. Res. B Appl. Biomater.* **2009**, *91B*, 930–937. [CrossRef]
40. Hallmann, L.; Ulmer, P.; Wille, S.; Polomskyi, O.; Kobel, S.; Trottenberg, T.; Bornholdt, S.; Haase, F.; Kersten, H.; Kern, M. Effect of surface treatments on the properties and morphological change of dental zirconia. *J. Prosthet. Dent.* **2016**, *115*, 341–349. [CrossRef]
41. Łagodzińska, P.; Dejak, B.; Krasowski, M.; Konieczny, B. The Influence of Alumina Airborne-Particle Abrasion with Various Sizes of Alumina Particles on the Phase Transformation and Fracture Resistance of Zirconia-Based Dental Ceramics. *Materials* **2023**, *16*, 5419. [CrossRef]
42. Li, M.; Xing, Y.; Zhu, C.; Liu, Q.; Yang, Z.; Zhang, R.; Zhang, Y.; Xia, Y.; Gui, X. Effect of roughness on wettability and floatability: Based on wetting film drainage between bubbles and solid surfaces. *Int. J. Min. Sci. Technol.* **2022**, *32*, 1389–1396. [CrossRef]
43. Mao, Y.; Xia, W.; Peng, Y.; Xi, G. Dynamic pore wetting and its effects on porous particle flotation: A review. *Int. J. Min. Sci. Technol.* **2022**, *32*, 1365–1378. [CrossRef]
44. Sandhu, R.; Kheur, M.; Kheur, S. Effect of simulated chairside grinding procedures using commercially available abrasive agents on the surface properties of zirconia. *J. Indian. Prosthodont. Soc.* **2017**, *17*, 22–28. [CrossRef] [PubMed]
45. Traini, T.; Gherlone, E.; Parabita, S.F.; Caputi, S.; Piattelli, A. Fracture toughness and hardness of a Y_TZP dental ceramic after mechanical surface treatments. *Clin. Oral Investig.* **2014**, *18*, 707–714. [CrossRef] [PubMed]
46. Maerten, A.; Zaslansky, P.; Mochales, C.; Traykova, T.; Mueller, W.D.; Fratzl, P.; Fleck, C. Characterizing the transformation near indents and cracks in clinically used dental yttria-stabilized zirconium oxide constructs. *Dent. Mater.* **2013**, *29*, 241–251. [CrossRef] [PubMed]
47. Subasi, M.G.; Inan, O. Evaluation of the topographical surface changes and roughness of zirconia after different surface treatments. *Lasers Med. Sci.* **2012**, *27*, 735–742. [CrossRef] [PubMed]
48. Hergeröder, C.; Wille, S.; Kern, M. Comparison of Testing Designs for Flexural Strength of 3Y-TZP and 5Y-PSZ Considering Different Surface Treatment. *Materials* **2022**, *15*, 3915. [CrossRef]

Disclaimer/Publisher's Note: The statements, opinions and data contained in all publications are solely those of the individual author(s) and contributor(s) and not of MDPI and/or the editor(s). MDPI and/or the editor(s) disclaim responsibility for any injury to people or property resulting from any ideas, methods, instructions or products referred to in the content.